Journal Name

ARTICLE TYPE

Cite this: DOI: 00.0000/xxxxxxxxxx

Tuning intrinsic ferromagnetic and anisotropic properties of Janus VSeS monolayer

Mahsa Abdollahi[a] and Meysam Bagheri Tagani*[a]

[a] *Computational Nanophysics Laboratory (CNL), Department of physics, University of Guilan, P. O. Box 41335-1914, Rasht, Iran.*

* *Corresponding Author, Email: m_bagheri@guilan.ac.ir*

Table 1 Structural parameters and magnetic moment of V-based monolayers : lattice constant, bond angle (θ_{S-V-Se}), bond length of V-S (d_{V-S}), V-Se (d_{V-Se}), and magnetic moment of V atom.

Monolayer	a (Å)	Θ_{X-V-Y} (deg)	d_{V-S} (Å)	d_{V-Se} (Å)	$m_V(\mu_B)$
VS_2	3.18	78.79	2.38	-	1.15
VSe_2	3.34	79.93	-	2.52	1.25
VSeS	3.24	79.61	2.37	2.52	1.16

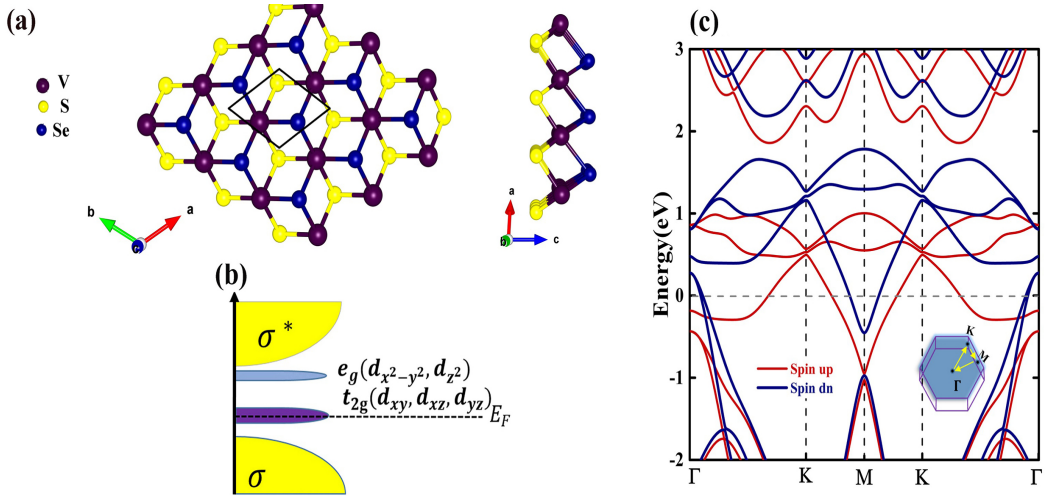

Fig. 1 Top and side view of (a) 1T-VSeS Janus monolayer with octahedral coordinate. The vanadium, selenide, and sulfur atoms are shown in purple, blue, and yellow, respectively. Unit cell is also identified.(b) Schematic illustration of Energy Splitting and Crystal Field (c) the spin-polarized band structure of 1T-VSeS.

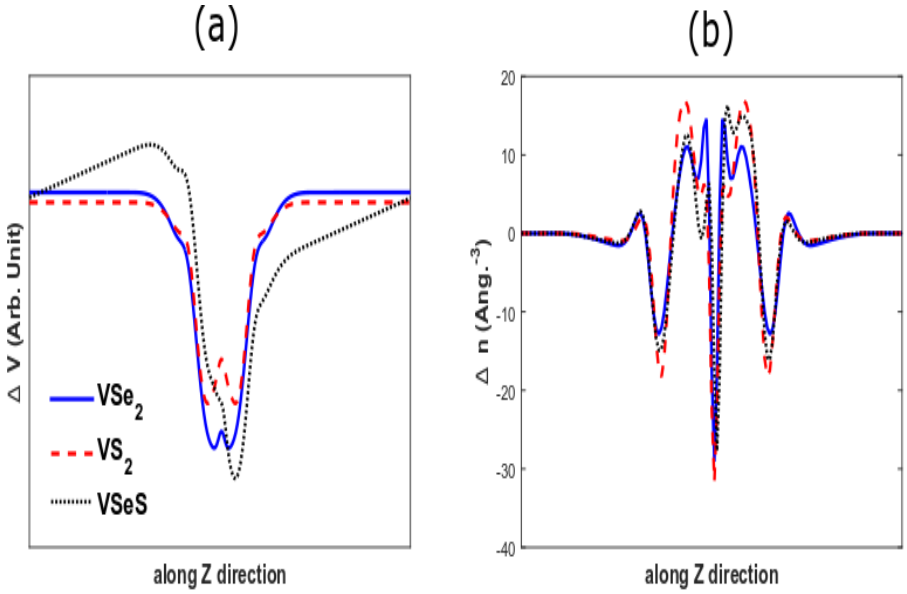

Fig. 2 (a) Potential difference, and (b) charge difference density along Z-direction for V-based monolayers.

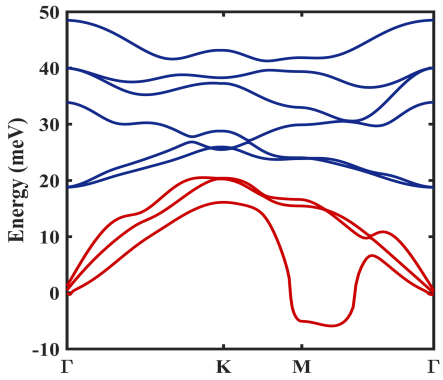

Fig. 3 Phonon band structure of NM VSeS monolayer. Blue (red) lines indicate optical (acoustic) phonon modes. The structure is dynamically unstable due to imaginary phonon modes around M point.

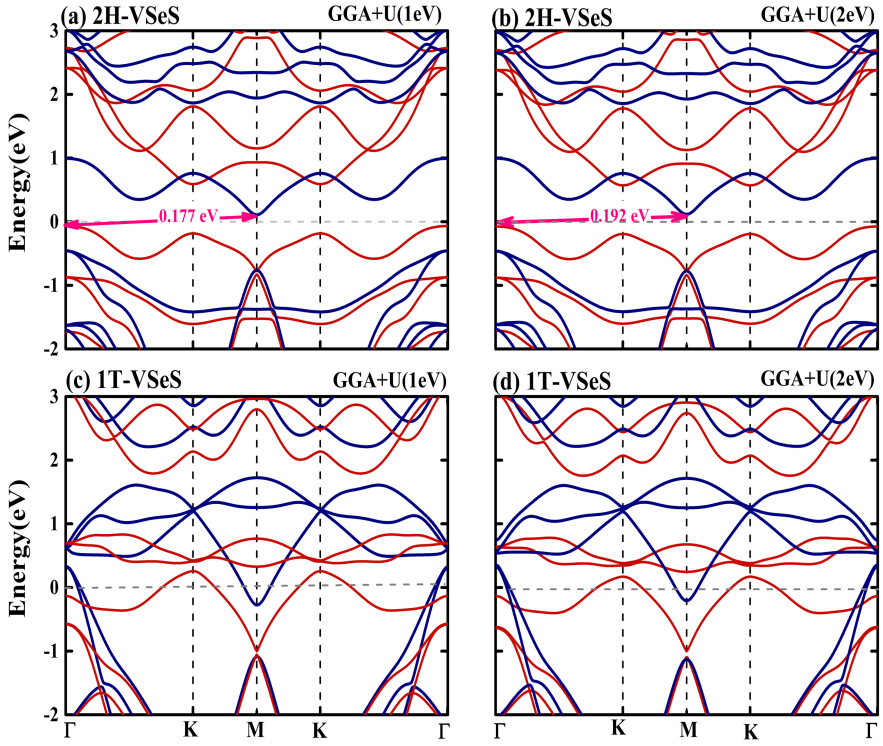

Fig. 4 Spin-polarized band structure for 2H(above) 1T(below) VSeS with Hubbard parameter (a),(c) U=1eV and (b)(d) U=2eV.

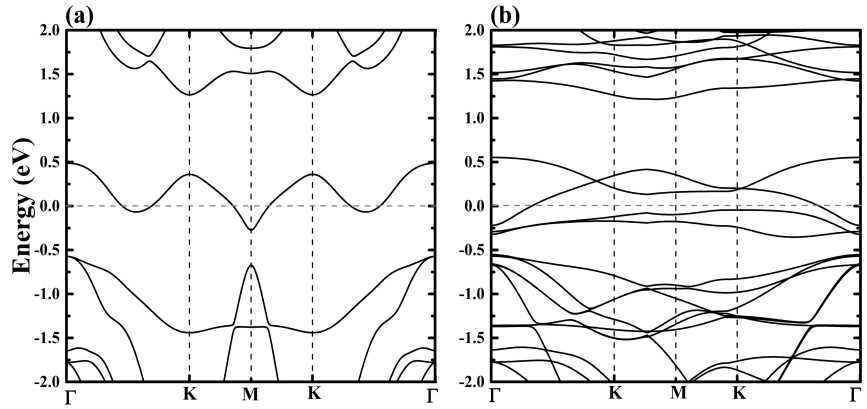

Fig. 5 Spin-polarized band structure for 2H-VSeS with (a) NM configuration (b) AFM configuration

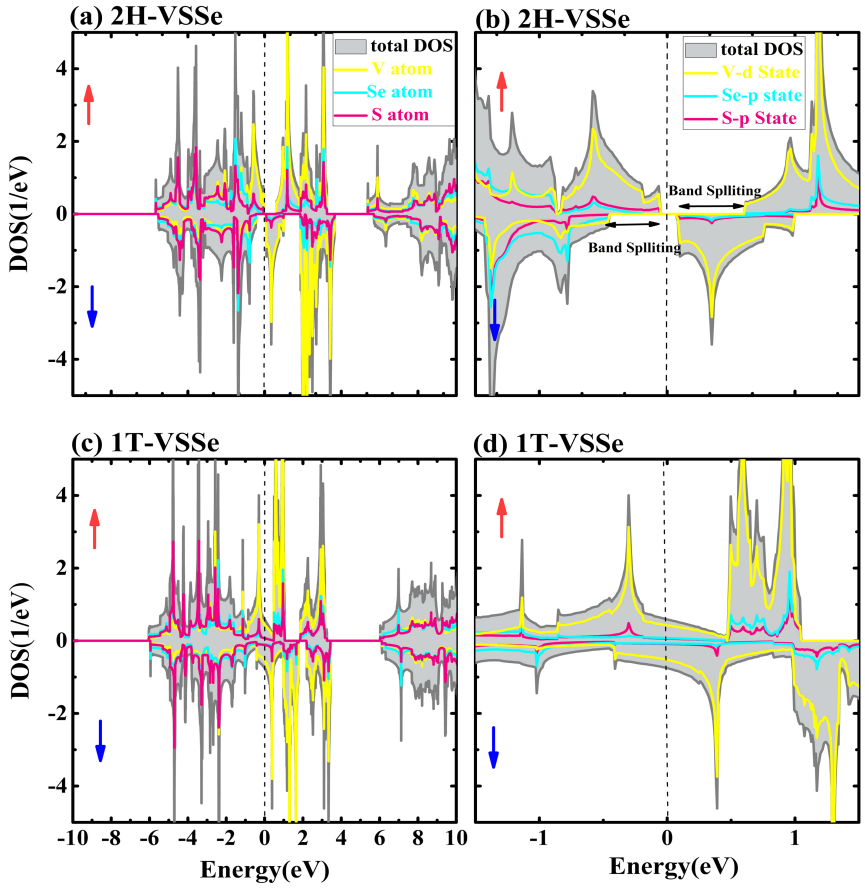

Fig. 6 spin-resolved density of states for atom (left) and orbital (right) state, (a), (b) 2H-VSeS (c), (d) 1T-VSeS.

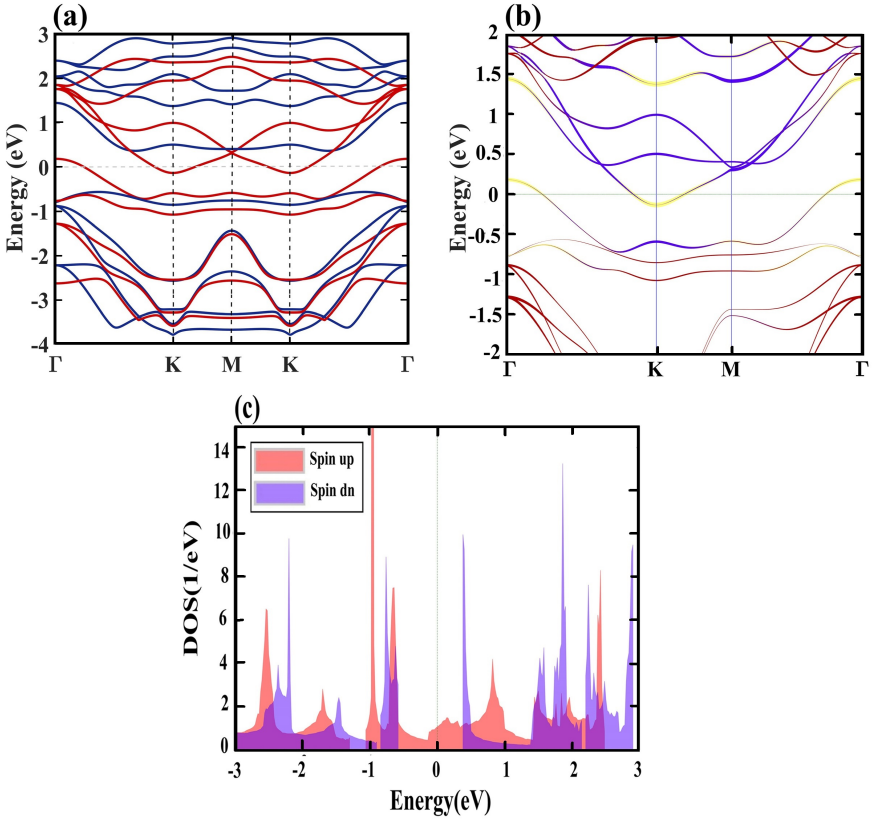

Fig. 7 (a) and (b) spin and orbital resolved band structure of the 2HVSeS monolayer under $\varepsilon = +10\%$. In (b) yellow, red, and blue lines denote d_{z^2}, (d_{xz}, d_{yz}), and $(d_{x^2-y^2}, d_{xy})$ orbitals, respectively. Spin-dependent density of states is shown in (c).

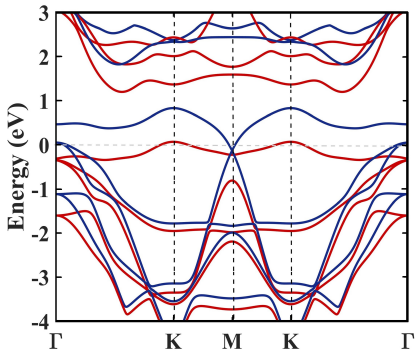

Fig. 8 Band structure of the monolayer under $\varepsilon = -6\%$. A Dirac point is observed for spin-down.

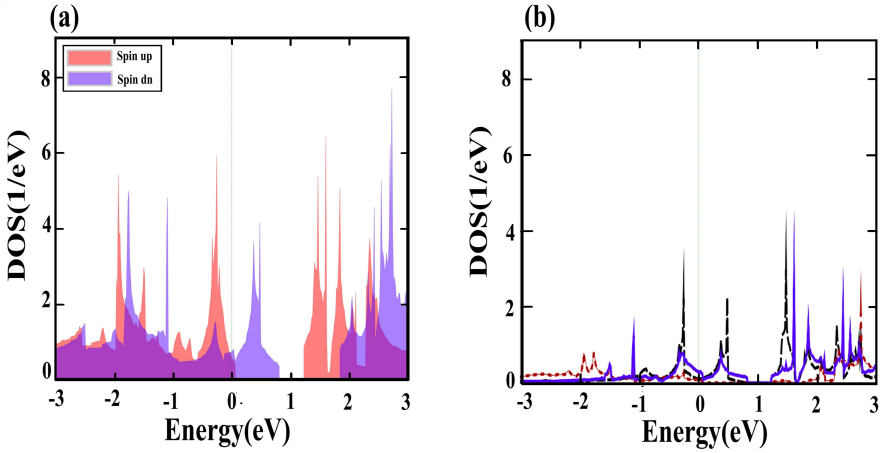

Fig. 9 (a) spin, (b) orbital resolved DOS of the monolayer under strain of $\varepsilon = -6\%$. Black, blue, and red lines show the contribution of d_{z^2}, $(d_{x^2-y^2}, d_{xy})$, and (d_{xz}, d_{yz}) orbitals, respectively.

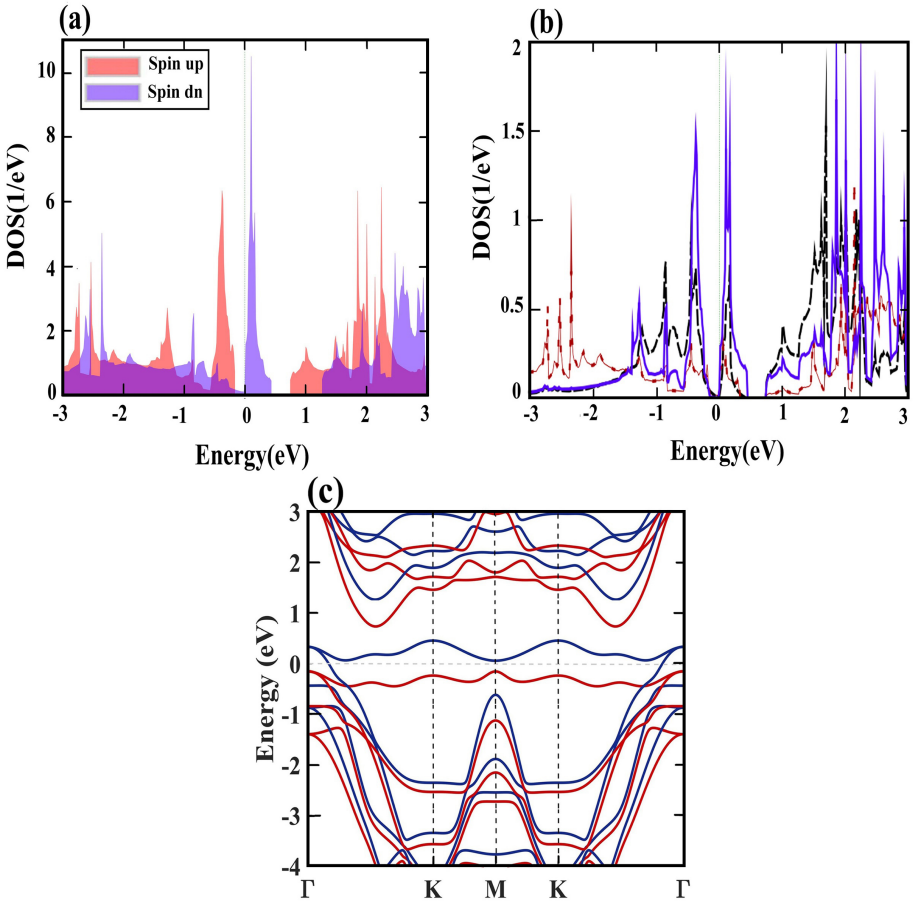

Fig. 10 (a) spin, (b) orbital resolved DOS of the monolayer under strain of $\varepsilon = -10\%$. Black, blue, and red lines show the contribution of d_{z^2}, $(d_{x^2-y^2}, d_{xy})$, and (d_{xz}, d_{yz}) orbitals, respectively. (c) spin-dependent band structure of the strained monolayer.

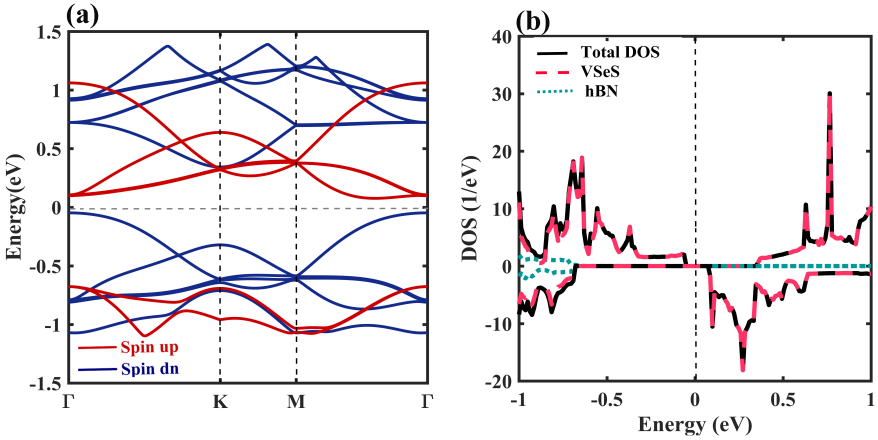

Fig. 11 (a) Band strauctures of the heterostructure in AFM configuration. (b) Density of states projected on each layer and spin for FM state. Fermi level is set to zero.